Article

Deep crustal assimilation during the 2021 Fagradalsfjall Fires, Iceland

https://doi.org/10.1038/s41586-024-07750-0

Received: 3 October 2023

Accepted: 25 June 2024

Published online: 31 July 2024

Check for updates

James M. D. Day[1]✉, Savannah Kelly[1], Valentin R. Troll[2,3], William M. Moreland[4], Geoffrey W. Cook[1] & Thor Thordarson[4]

Active basaltic eruptions enable time-series analysis of geochemical and geophysical properties, providing constraints on mantle composition and eruption processes[1–4]. The continuing Fagradalsfjall and Sundhnúkur fires on Iceland's Reykjanes Peninsula, beginning in 2021, enable such an approach[5,6]. Earliest lavas of this volcanic episode have been interpreted to exclusively reflect a change from shallow to deeper mantle source processes[7]. Here we show using osmium (Os) isotopes that the 2021 Fagradalsfjall lavas are both fractionally crystallized and strongly crustally contaminated, probably by mid-ocean-ridge gabbros and older basalts underlying the Reykjanes Peninsula. Earliest eruptive products ($^{187}Os/^{188}Os \leq 0.188$, platinum (Pt)/iridium (Ir) ≤ 76) are highly anomalous for Icelandic lavas or global oceanic basalts and Os isotope ratios remain elevated throughout the 2021 eruption, indicating a continued but diluted presence of contaminants. The 2022 lavas show no evidence for contamination ($^{187}Os/^{188}Os = 0.131$, Pt/Ir = 30), being typical of Icelandic basalts (0.132 ± 0.007). Initiation of the Fagradalsfjall Fires in 2021 involved pre-eruptive stalling, fractional crystallization and crustal assimilation of earliest lavas. An established magmatic conduit system in 2022 enabled efficient magma transit to the surface without crustal assimilation.

On 19 March 2021, a new eruption period began on the Reykjanes Peninsula, Iceland after 781 years of volcanic quiescence[5–7]. The Reykjanes Peninsula represents the southwestern-most manifestation of subaerial eruption in Iceland, at which the Mid-Atlantic Ridge intersects with an anchored and deeply derived mantle plume[8–11] (Fig. 1). Volcanic activity along the Reykjanes Peninsula has been characterized by several 300-to-500-year eruption periods followed by 600-to-1,000-year repose times[12]. Initiation of basaltic volcanism and the tempo of eruption within notable eruption periods, for both Iceland and globally[3,4], however, remain poorly understood. The recent eruptions of the Fagradalsfjall Fires, named for the hyaloclastite complex within which the initiation of renewed volcanism took place, are critical for understanding the causes and consequences of long-term basaltic volcanic events. So far, the Fagradalsfjall Fires have included three eruptive events; the 2021 Geldingadalir eruption lasting for 183 days (19 March to 18 September), the 2022 Meradalir eruption lasting 18 days (3 to 21 August) and the 2023 Litli-Hrútur eruption that began on 10 July and ended by 5 August (26 days), all focused on the Fagradalsfjall hyaloclastite ridge (Fig. 1). Most recently, the Sundhnúkur eruptions have taken place near Grindavik, with four discrete eruptions along the Sundhnúkurgigar fissure system from 18 to 21 December 2023 (3 days), 14 to 15 January 2024 (2 days), 8 February 2024 (1 day) and 16 March 2024 (54 days).

Volcanic eruption time-series monitoring

A feature of the Fagradalsfjall Fires is the ability to undertake time-series monitoring of the geochemical and geophysical properties of the eruption event[5,7,13]. It has been proposed that magmas feeding the 2021 eruptive episode were directly sourced from a near-Moho magma storage zone and underwent an evolution from contributions of shallow, depleted mantle melts to more deeply derived, enriched mantle melts[7]. Magmas were interpreted as uncompromised by hydrothermally altered shallow crust[5], despite evidence for prolonged (up to one year) storage before mobilization that led to the start of the 2021 eruptive episode[14,15]. To understand the recorded geochemical variations at the initiation of the Fagradalsfjall Fires more fully, and to resolve the apparently contradicting models and observations of closed-system storage and pre-eruptive crustal magma residence versus directly sourced mantle fed eruptions, we examined lavas from the 2021 Geldingadalir and 2022 Meradalir eruptions for precise compatible and incompatible trace-element data, including highly siderophile element (HSE: Re, Pd, Pt, Ru, Ir, Os) abundances and $^{187}Re–^{187}Os$ systematics (Supplementary Data Table 1). The Re–Os isotope system has recently been shown to be a particularly powerful radiogenic isotope tool for understanding changes in magma chemistry during basaltic eruptions[16]. This is because of its sensitivity to assimilation of high Re/Os basaltic materials that develop radiogenic $^{187}Os/^{188}Os$, material that other isotope systems

[1]Scripps Institution of Oceanography, University of California San Diego, La Jolla, CA, USA. [2]Department of Earth Sciences, Natural Resources and Sustainable Development (NRHU), Uppsala University, Uppsala, Sweden. [3]Centre of Natural Hazards and Disaster Science (CNDS), Uppsala University, Uppsala, Sweden. [4]Faculty of Earth Sciences, University of Iceland, Reykjavík, Iceland. ✉e-mail: jmdday@ucsd.edu

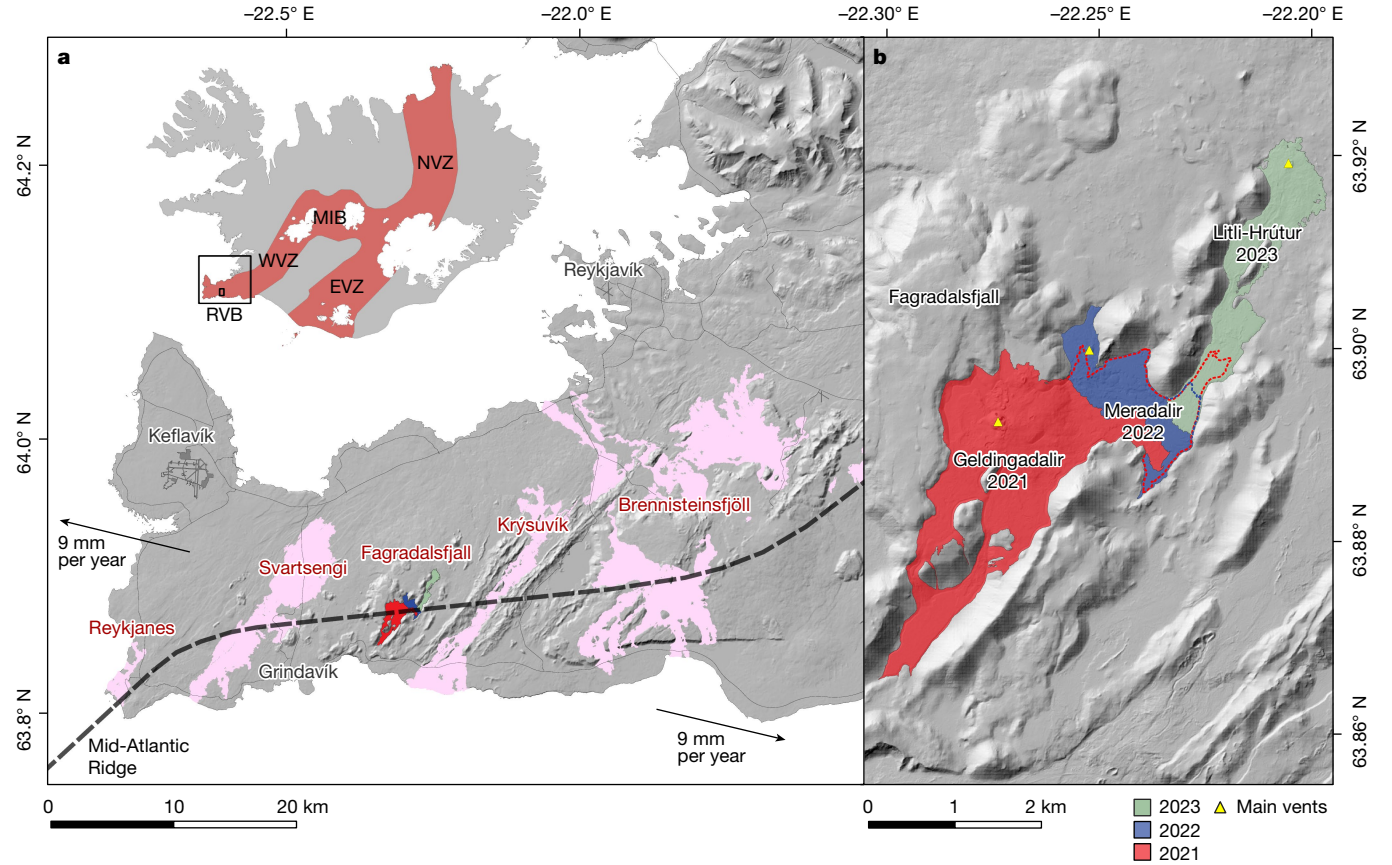

Fig. 1 | Location map of the Fagradalsfjall Fires that began in March 2021, showing the 2021, 2022 and summer 2023 episodes. a, The broader setting of the Reykjanes Peninsula. **b**, 2021–2023 Fagradalsfjall Fires. The most recent Sundhnúkur eruptions occurred northwest of Grindavik. Background digital elevation model with roads and airports is the 2-m ÍslandsDEM from Landmælingar Íslands (National Land Survey of Iceland). The 2021 lava outline is from ref. 37, with plate-spreading velocity from refs. 12,38. Outlines of the 2022 and 2023 lavas from ref. 13 and underlying digital elevation models for those lava fields are new to this study. EVZ, Eastern Volcanic Zone; MIB, Mid-Iceland Belt; NVZ, Northern Volcanic Zone; RVB, Reykjanes Volcanic Belt; WVZ, Western Volcanic Zone.

are unable to unambiguously detect (for example, Sr–Nd–Pb)[16]. As a complimentary geochemical tool, HSE abundances provide information on crystal–liquid fractionation processes[16].

Rhenium–osmium isotopes and HSE abundance analyses were performed on samples from the 2021 and 2022 eruption periods in two analytical campaigns. Rock fragments were prepared at Scripps Institution of Oceanography, where sample powders were prepared using an alumina crusher and shatterbox. Detailed descriptions of the analytical methods used in this study are provided in Methods and follow previous work[16]. In brief, bulk rock minor-element and trace-element abundance data were determined to obtain precise determination of Ni contents, a useful proxy for estimating HSE abundances in lavas. Following these measurements, nine, four and six samples that span the eruptions were selected from days 1–51 and 125–160 of the 2021 eruption and from the 2022 eruption, respectively.

Geldingadalir 2021 and Meradalir 2022 eruptive products are basalts with similar average MgO contents (9.0 ± 1.0 wt% (n = 24) and 9.0 ± 0.5 wt% (n = 22); all at 2 s.d.), with the largest variability between days 1 and about 51 of the 2021 eruption, which also have the lowest MgO (Fig. 2a). Compatible elements co-vary with MgO, with Ni contents increasing from 121 to 203 μg g^{-1} during the 2021 eruption and ranging from 124 to 156 μg g^{-1} during the 2022 eruption. Incompatible trace elements are either invariant during the eruptions (for example, heavy rare earth elements, V, Li, Zr) or increase from day 1 to 51 of the 2021 eruption, with 2022 basalts having elevated abundances of these elements similar to or greater than basalts erupted at the end of 2021, with K_2O/TiO_2 increasing from the start of 2021 and being highest in the 2022 eruption products (Fig. 2b). In this regard, the Fagradalsfjall Fires have highly distinct trace-element ratios to Holocene lavas erupted on the Reykjanes Peninsula[5,7]. Ratios of Zr/Hf (37.3 ± 1.0 and 37.8 ± 0.6, respectively) and Nb/Ta (16.1 ± 0.4 and 16.3 ± 0.3, respectively) are within the range of canonical values for ocean island basalts (OIB)[17]. In turn, La/Yb (3.3 ± 0.7 and 4.5 ± 0.3, respectively) and Ce/Pb (24 ± 7 and 32 ± 2, respectively) are lower and more variable in 2021 Geldingadalir versus 2022 Meradalir basalts, with the 2022 sample suite being more similar to enriched central Iceland lavas[18] than to the most highly depleted Icelandic tholeiite compositions[19]. Ratios of La/Sm, La/Y and Sr/Zr closely track variations of La/Yb, indicating a coherence of incompatible trace-element ratios in the Fagradalsfjall Fire lavas.

Abundances of Os show no systematic variation with day of eruption for the Fagradalsfjall Fires, ranging from 0.044 to 0.32 ng g^{-1}. Abundances of Pt, Pd and Re are at generally higher concentrations at the beginning of 2021 than at the end of eruption in 2021 or in 2022. Ratios of Pt/Ir and Re/Os are highest during the onset of the 2021 eruption and decrease after the second week of the 2021 eruption, into 2022 (Fig. 2c). Notably, measured $^{187}Os/^{188}Os$ for the initial phase of the 2021 eruption are highly radiogenic (up to 0.188, average = 0.152 ± 0.036, 2 s.d.)—far more radiogenic than any previously reported Icelandic basalt with >50 pg g^{-1} Os (Fig. 2d and Extended Data Fig. 1). The $^{187}Os/^{188}Os$ oscillates between ratios similar to typical Icelandic basalts to radiogenic ratios from day 1 to 51 of 2021, reverting to consistently radiogenic $^{187}Os/^{188}Os$ from day 125 to 160 of 2021 (0.1415 ± 0.0082; 2 s.d.). The 2022 Meradalir eruptive products have similar $^{187}Os/^{188}Os$ (0.1307 ± 0.0047; 2 s.d.) to

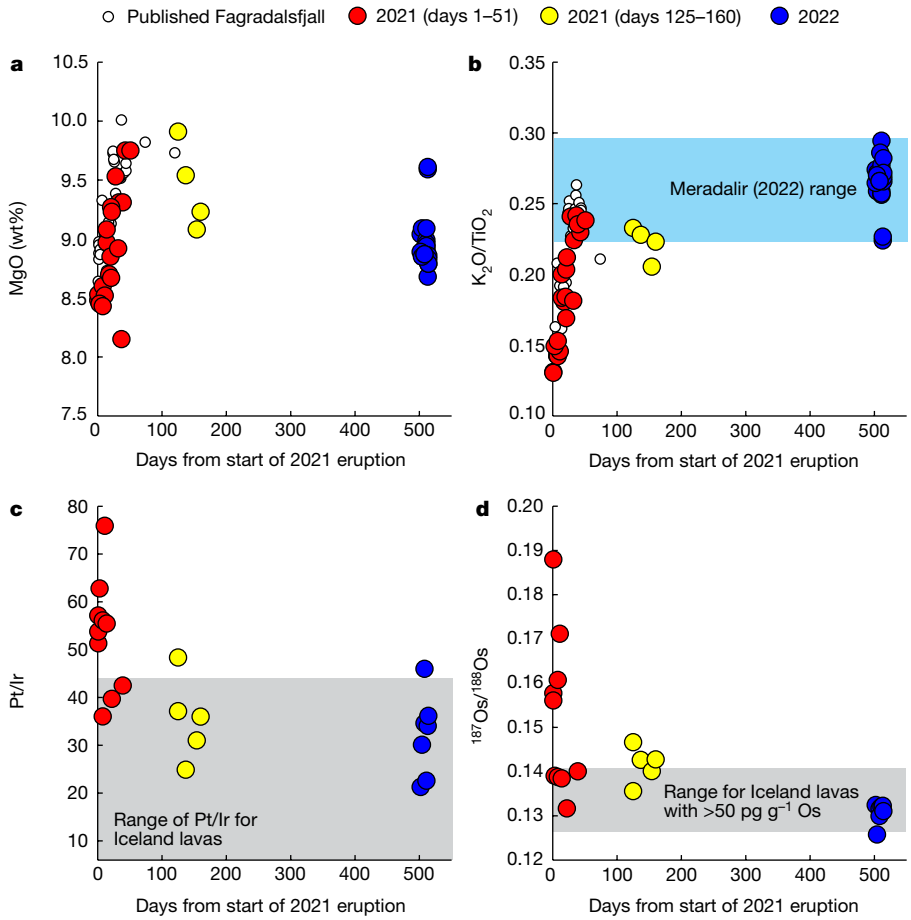

Fig. 2 | Geochemical variations in lavas from the 2021 and 2022 Iceland eruptions as a function of the day of their emplacement, beginning on 19 March 2021. Variations shown are days since eruption versus MgO (**a**), K_2O/TiO_2 (**b**), Pt/Ir (**c**) and measured $^{187}Os/^{188}Os$ (**d**). Previously published data for the first 50 days of the Geldingadalir eruption of 2021 are from ref. 7. Range of Pt/Ir for Iceland picrites are from refs. 39,40 and range of Os isotope variations are from data sources listed in the Supplementary Information. Uncertainties on X-ray fluorescence and inductively coupled plasma mass spectrometry measurements are less than 2% relative and about 5% relative, respectively (see Supplementary Data Table 1).

previously published Iceland basalt compositions (0.132 ± 0.007; 2 s.d.; Fig. 2d). Lavas from the 2021 eruption with the lowest Os contents typically have the most radiogenic $^{187}Os/^{188}Os$, whereas lavas from the 2022 eruption have relatively invariant $^{187}Os/^{188}Os$ for a similar range of Os abundances (Extended Data Fig. 1).

Initial 2021 (Geldingadalir) lavas of the Fagradalsfjall Fires generally have highly radiogenic $^{187}Os/^{188}Os$ (0.1316–0.1879) coupled with high Pt/Ir (25–76) and $^{187}Re/^{188}Os$ (7–67). By contrast, the 2022 Meradalir lavas have compositions of $^{187}Os/^{188}Os$ from 0.1258 to 0.1324, Pt/Ir from 21 to 46 and $^{187}Re/^{188}Os$ from 5 to 21. These trends in Os isotope and HSE abundance data are associated with changing major-element and trace-element abundance compositions for the 2021 eruption, from generally lower MgO abundances and incompatible element ratios ($K_2O/TiO_2 \geq 0.12$, La/Yb ≥ 2.2) to higher MgO and higher K_2O/TiO_2 (≥0.25) and La/Yb (≥4.1). For incompatible trace elements, the 2022 Meradalir lavas are similar to the latest 2021 lavas, but trend to generally lower MgO. For the later 2021 and the 2022 lavas, their compositions are consistent with deriving from more limited fractional crystallization of MgO-rich parental magmas compared with the day 1–51 lavas, with fractionation of olivine explaining the range of Ni contents (Fig. 3a) and fractionation of approximately 10% olivine and minor sulfide explaining the HSE abundances and increasing Pt/Ir owing to S saturation of the parental magmas (Extended Data Fig. 2). The geochemical systematics set the Fagradalsfjall Fires apart from earliest contaminated products of continental flood basalts, which are related to assimilation of fusible components by hot primitive magmas[20,21].

Evidence for deep crustal assimilation

Fractional crystallization alone cannot explain the highly radiogenic Os isotope compositions in the earliest portions of the 2021 eruption (Fig. 3b). The time-series data for the lavas show initially radiogenic $^{187}Os/^{188}Os$ and high Pt/Ir in the most incompatible element-depleted melts, changing to more incompatible element-rich melts with typical Icelandic basalt $^{187}Os/^{188}Os$ and Pt/Ir ratios (Fig. 4a,b). These isotope and abundance systematics are completely unexpected. Initial interpretation was that lavas were not substantially contaminated by low-$\delta^{18}O$ Icelandic crust[5] and that the earliest lavas reflected melting of depleted mantle sources, with later lavas reflecting tapping of progressively more enriched and possibly deeper mantle sources[7]. The most radiogenic primitive Os isotope compositions of oceanic lavas with >50 pg g^{-1} Os measured so far[22], however, are exceeded in values by those observed in the 2021 Fagradalsfjall Fires lavas. These highly radiogenic compositions at the start of the Fagradalsfjall Fires cannot be explained by enhanced contributions of metasomatized Archaean continental lithospheric mantle, which produces unradiogenic $^{187}Os/^{188}Os$ (for example, ref. 23). Nor can these signatures be explained by enriched mantle sources such as HIMU or pelagic sediments, which would have $^{206}Pb/^{204}Pb$ too high and $^{143}Nd/^{144}Nd$ too low, respectively, to explain the 'depleted' early lavas of the 2021 Fagradalsfjall Fires[7]. Instead, the new Os isotope data provide incontrovertible evidence for contamination by crustal assimilation of original mantle-derived magmas and thus negate the concept of magma ascent directly from the mantle for the initial phase of the 2021 eruption.

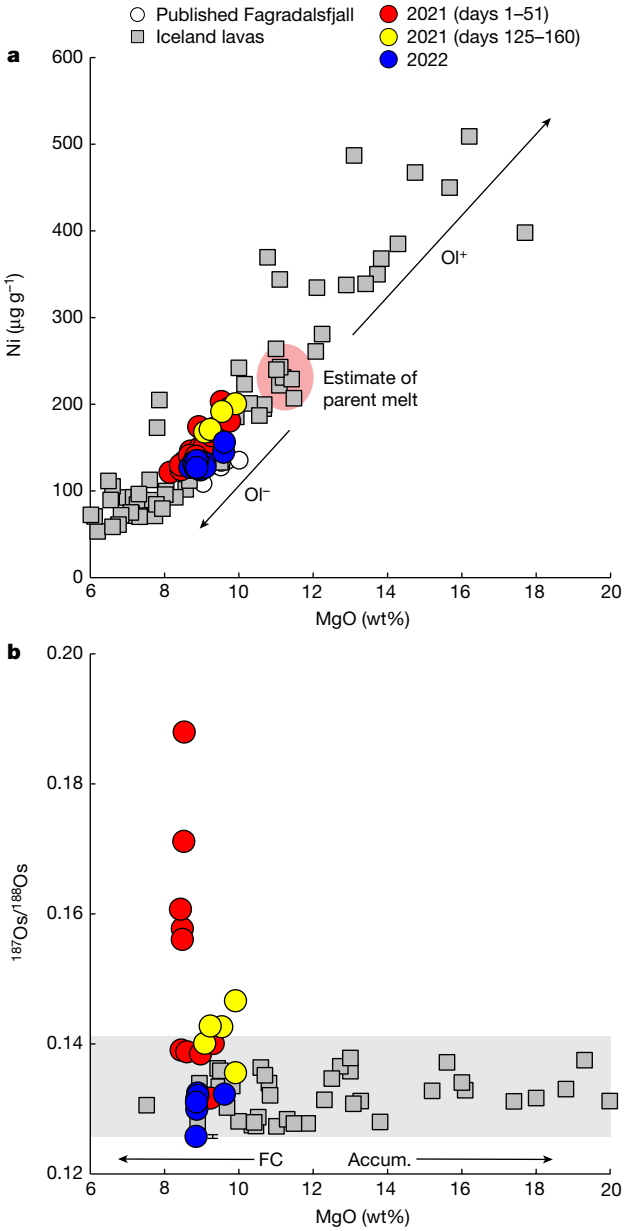

Fig. 3 | Illustration of processes acting on Fagradalsfjall magmas from MgO versus Ni and $^{187}Os/^{188}Os$. a, MgO versus Ni. **b**, MgO versus $^{187}Os/^{188}Os$. Fagradalsfjall lavas show fractional crystallization trends of low Ni and MgO, with 2022 lavas having marginally lower Ni for a given MgO content. Osmium isotope data for 2022 Fagradalsfjall lies within the range of previous Icelandic lavas, with 2021 lavas extending well beyond the typical range observed in Iceland. Parent melt estimate in **a** from ref. 19 and published data are given in the Supplementary Information. Accum., accumulation; FC, fractional crystallization.

Models of shallow crust assimilation can explain the oxygen trace element (Extended Data Fig. 3) and O–Os isotope systematics of previously reported Icelandic basalts and picrites (Fig. 4d) but suggest no shallow crustal assimilation in 2021 and 2022 eruptive products at Fagradalsfjall, consistent with previous results[5]. Deep crust assimilation (approximately 10–15 km), however, would occur at relatively high temperatures (>800 °C), at which hydrothermal alteration and associated fluid flow is extremely unlikely and is consistent with pooling of the earliest magmas for up to a year at such depths[14]. Such deep crustal assimilation also precludes a direct effect from seawater, which otherwise has radiogenic $^{187}Os/^{188}Os$ but low Os contents. Conversely, it is impossible to reconcile the radiogenic Os isotopes in the context of models invoking depleted to enriched mantle sources with time during the Fagradalsfjall Fires, as proposed by ref. 7. Our expectation, based on a change from more depleted to enriched signatures for Sr–Nd–Pb isotopes and trace-element chemistry at the start of the 2021 eruption[7], was to measure less radiogenic Os isotope compositions in 'depleted' lavas during the earliest stages of the eruption, followed by more radiogenic Os later in the eruption. This would be consistent with knowledge from long-term Re–Os isotope systematics in depleted and enriched mantle sources[22]. However, the opposite has proved the case, compelling us to radically reinterpret the petrogenetic model of the lavas erupted during the Fagradalsfjall Fires.

Identifying sources of radiogenic osmium

To explore the role of crustal assimilation, we constrain assimilation and fractional crystallization (AFC) to the crust–mantle boundary (about 10–15 km), consistent with geophysics[24] and barometry[7,25]. On the basis of predicted densities[24], the expected crustal lithologies in contact with mantle peridotite at the Moho are probably gabbroic and basaltic rocks. So far, no oceanic peridotites have been shown to have radiogenic $^{187}Os/^{188}Os$, although some incompatible element-enriched pyroxenite veins have been reported with $^{187}Os/^{188}Os$ up to 0.146 (ref. 26). It is therefore highly improbable that the radiogenic signatures of the early 2021 Fagradalsfjall Fires lavas were the result of interaction with oceanic mantle lithosphere.

Oceanic crustal rocks, including gabbro and basaltic rocks, can extend to very radiogenic $^{187}Os/^{188}Os$ (about 1) over short time periods (about 10 million years ago (Ma)) by virtue of having high $^{187}Re/^{188}Os$ (up to 1,300) and are also characterized by high Pt/Ir (>30)[27,28]. An impediment to such rocks being potential crustal contaminants to the earliest 2021 lavas is that the Reykjanes Peninsula lies on young crust along a plate boundary, with half-plate speeds of roughly 9.3 mm per year (ref. 6), suggesting that underlying lithosphere is probably not more than a few million years old. Alternatively, it has been proposed that ancient recycled oceanic crust may be present in the deep Icelandic mantle[18,19] or that slivers of pre/syn-breakup oceanic and older continental crust may occur under parts of Iceland[29,30].

We explored basic AFC models for assimilation to explain the high $^{187}Os/^{188}Os$ of the earliest Fagradalsfjall Fire lavas (Fig. 4c). A key aspect of these models is that, although the trace elements of the earliest eruptive products are depleted, the $^{187}Os/^{188}Os$ in these lavas are anomalously radiogenic for Iceland. There are strong correlations with trace-element ratios (for example, La/Yb, La/Sm, La/Y, Sr/Zr) with $^{187}Os/^{188}Os$ but not with Eu anomalies, suggesting complex assimilation and fractional crystallization acting of parent magmas. Preferential sampling by the earliest 2021 lavas of recycled oceanic crust or a continental crustal sliver in the Iceland plume can be ruled out based on the models. As well as such a contribution violating the incompatible element-depleted nature of the earliest lavas, the likely composition of ancient recycled oceanic gabbro or basalt[19,31] is unlikely to produce the Pt/Ir and $^{187}Os/^{188}Os$ systematics observed in the Fagradalsfjall Fires lava products, even if concomitant with fractional crystallization (Fig. 4c, model i).

Another possibility that we explored is that ponding of hot-mantle-derived melts at the Moho led to preferential melting of high Re/Os and Pt/Ir sulfides or of fractional fusion melting of gabbros. In this model, sulfides or S-rich gabbros formed as much as 10 Myr ago are assumed to have occurred. Comparison of data for base metal sulfides from ocean ridges and other tectonic settings show, however, that these published compositions are not likely candidates for the radiogenic Os observed in the earliest Fagradalsfjall lavas. In extreme circumstances, they can produce high Pt/Ir but are unable to produce radiogenic $^{187}Os/^{188}Os$ in 10 Ma or less (Fig. 4c). For sulfides to be potential contaminants beneath the Reykjanes Ridge, they would require

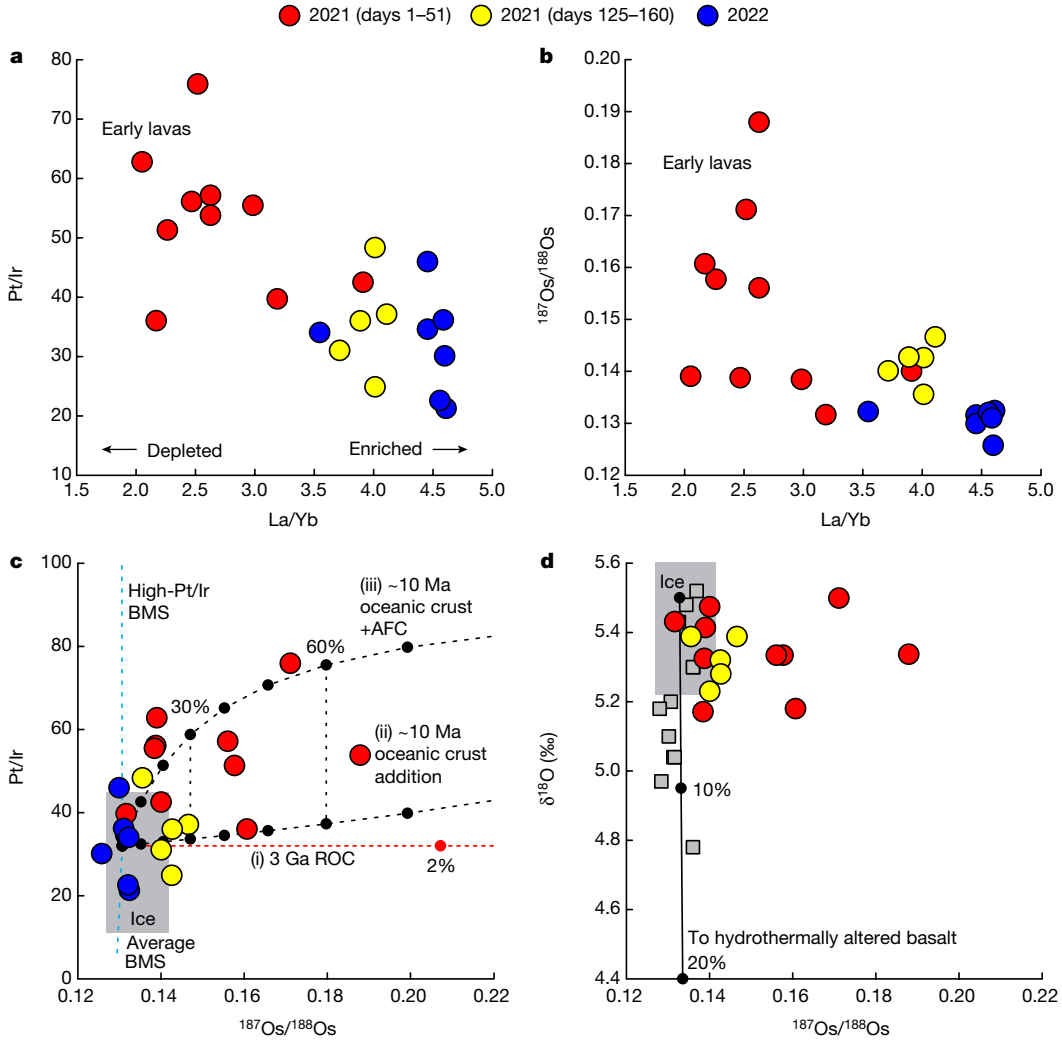

Fig. 4 | Plots of La/Yb versus Pt/Ir and $^{187}Os/^{188}Os$ and Os isotopes versus Pt/Ir and $\delta^{18}O$ for the 2021 and 2022 Fagradalsfjall Fires. a, La/Yb versus Pt/Ir. **b**, La/Yb versus $^{187}Os/^{188}Os$. **c**, Os isotopes versus Pt/Ir. **d**, Os isotopes versus $\delta^{18}O$. Shown in **a** are interpretations of enriched and depleted melts based on La/Yb and shown in **d** is a mixing model between typical Icelandic melts and hydrothermal altered basalt. **c**, Model curves corresponding to mixing between the average melt from the high-MgO 2022 lavas of the Fagradalsfjall Fires and: (i) 3 Ga recycled oceanic crust (ROC); (ii) roughly 10 Ma oceanic crust (gabbro); (iii) AFC during assimilation of approximately 10 Ma gabbro. Also shown are the models of Os mixing with average base metal sulfides (BMS) aged for 10 Ma and anomalous high-Pt/Ir BMS. For model parameters, see Supplementary Data Table 3. Published Iceland data in grey squares in **d** from ref. 19 (Os) and ref. 34 (O).

extremely high Re/Os ($^{187}Re/^{188}Os > 5{,}000$) and no such contaminants have yet been identified.

Models assuming solely AFC include the addition of relatively recently formed (10 Ma) oceanic crust beneath the Reykjanes Peninsula. The presented AFC models are a first-order approximation and are not thermodynamically constrained and do not account for wall rock partial melting dynamics, which can enhance transfer of incompatible trace-element abundances from the assimilant[32]. Consequently, the 20% and 60% assimilation from our models are probably an overestimation and will only be improved by constraints on likely assimilants beneath the Reykjanes Peninsula. These models nevertheless illustrate that AFC can explain the variations in Os isotopes, HSE abundances and trace elements for the early 2021 lavas (Fig. 4c, models ii and iii). Elevated quantities of assimilation are not unreasonable when melts reside in contact with old (>1 Ma) mid-ocean ridge basalt (MORB) type wall rock within the lower crust, at which year-long residence times[14] and high temperatures could also have resulted in remobilization of MORB mush material during reactive flow (for example, ref. 33). Critically, AFC can explain the unradiogenic $^{206}Pb/^{204}Pb$, $^{87}Sr/^{86}Sr$ and radiogenic $^{143}Nd/^{144}Nd$ in the early 2021 lavas and the mantle-like oxygen isotopes[5,7]. Assimilation of MORB-like sources (Extended Data Fig. 4) would concomitantly lead to relatively limited effects on major-element bulk composition. If the later 2022 lavas did not experience the same degree of oceanic gabbro crustal assimilation, it would also explain why the 2021 lavas have uniformly higher $^{187}Os/^{188}Os$ but uniformly lower K_2O/TiO_2 than the 2022 lavas (Fig. 2).

Magma storage and eruption dynamics

The new Os isotope and HSE abundance data for the Fagradalsfjall Fires provide irrefutable evidence for crustal assimilation within a young magmatic setting. The notable range in $^{187}Os/^{188}Os$ for the Fagradalsfjall Fires exceeds the range found for OIB globally[34] and follows a similar, albeit more extreme, trend to the 2021 eruption of Tajogaite volcano on La Palma, Canary Islands[16]. There the earliest erupted lavas were more differentiated and contaminated by radiogenic crustal components, whereas later lavas were more primitive and returned to 'average' $^{187}Os/^{188}Os$ for La Palma lavas[16]. The evidence for contamination

by crustal assimilation in magmas before the onset of notable basaltic eruptions may suggest stalling and difficulty for earliest magmas in breaking through to the surface until tectonic unrest and may be an important feature for understanding eruption triggering. Assimilation of crust and concomitant fractional crystallization will act to increase volatile abundances (for example, CO_2 and SO_2) in melts, increasing internal pressures associated with the magma and reduce melt densities (for example, ref. 35), which will increase buoyancy. We suggest that crustal assimilation at the onset of new basaltic eruptions may be common during the development of new magma transit pathways through the crust. Indications are that ponded magma portions were remobilized and transported to the surface in conjunction with later injections from depth or by tectonic opening of crustal pathways that permitted magma ascent. Critically, the earliest erupted magmas in such scenarios may not be well suited for assessing mantle compositions.

Unlike the early 2021 lavas, the 2022 Meradalir eruption of the Fagradalsfjall Fires trend to relatively incompatible element-enriched compositions, similar to some Miocene northwest Iceland (SEL 97; ref. 10) and central Icelandic picrites with high $^3He/^4He$ (>30R_A; NAL 625; ref. 18). This not only suggests an enriched component that may occur in Reykjanes lavas but illustrates the potential for an evolving magma transit system through the Icelandic crust from the onset to maturation of eruption episodes. Initial deep crustal assimilation of lavas in 2021 was not repeated in 2022, consistent with an established and lined conduit for magma migration to the surface. This indicates shielding of later magmas from crustal assimilation and/or more efficient magma transit through the crust through such established and lined conduits and pathways. The ubiquitous evidence for assimilation of hydrothermally altered basalt into central Icelandic lavas might also suggest efficient magma transit through the deep crust and later stalling in the shallow crust[18,36], a feature also observed in some prehistoric Reykjanes Peninsula lavas[34]. Predictive power in these interpretations indicates that initial fractional crystallization and assimilation before the onset of basaltic volcanism is probably a function of a gradual build-up of magma within a larger volcanic system under the Reykjanes Peninsula, that—when released by tectonic movements—may characterize the initial stages of a long-lived and continuing episode of volcanic activity.

Online content

Any methods, additional references, Nature Portfolio reporting summaries, source data, extended data, supplementary information, acknowledgements, peer review information; details of author contributions and competing interests; and statements of data and code availability are available at https://doi.org/10.1038/s41586-024-07750-0.

1. Self, S., Thordarson, T. & Widdowson, M. Gas fluxes from flood basalt eruptions. *Elements* **1**, 283–287 (2005).
2. Thordarson, T. & Self, S. The Laki (Skaftár fires) and Grímsvötn eruptions in 1783–1785. *Bull. Volcanol.* **55**, 233–263 (1993).
3. Carracedo, J. C., Badiola, E. R. & Soler, V. The 1730–1736 eruption of Lanzarote, Canary Islands: a long, high-magnitude basaltic fissure eruption. *J. Volcanol. Geotherm. Res.* **53**, 239–250 (1992).
4. Garcia, M. O., Pietruszka, A. J., Rhodes, J. M. & Swanson, K. Magmatic processes during the prolonged Pu'u 'O'o eruption of Kilauea Volcano, Hawaii. *J. Petrol.* **41**, 967–990 (2000).
5. Bindeman, I. N. et al. Diverse mantle components with invariant oxygen isotopes in the 2021 Fagradalsfjall eruption, Iceland. *Nat. Commun.* **13**, 3737 (2022).
6. Sigmundsson, F. et al. Deformation and seismicity decline before the 2021 Fagradalsfjall eruption. *Nature* **609**, 523–528 (2022).
7. Halldórsson, S. A. et al. Rapid shifting of a deep magmatic source at Fagradalsfjall volcano, Iceland. *Nature* **609**, 529–534 (2022).
8. Schilling, J. G. Iceland mantle plume: geochemical study of Reykjanes Ridge. *Nature* **242**, 565–571 (1973).
9. Wolfe, C. J., Bjarnason, I., VanDecar, J. C. & Solomon, S. C. Seismic structure of the Iceland mantle plume. *Nature* **385**, 245–247 (1997).
10. Hilton, D. R., Grönvold, K., Macpherson, C. G. & Castillo, P. R. Extreme $^3He/^4He$ ratios in northwest Iceland: constraining the common component in mantle plumes. *Earth Planet. Sci. Lett.* **173**, 53–60 (1999).
11. Murton, B. J., Taylor, R. N. & Thirlwall, M. F. Plume–ridge interaction: a geochemical perspective from the Reykjanes Ridge. *J. Petrol.* **43**, 1987–2012 (2022).
12. Sæmundsson, K., Sigurgeirsson, M. Á. & Friðleifsson, G. Ó. Geology and structure of the Reykjanes volcanic system, Iceland. *J. Volcanol. Geotherm. Res.* **391**, 106501 (2020).
13. Krmíček, L., Troll, V. R., Galiová, M. V., Thordarson, T. & Brabec, M. Trace element composition in olivine from the 2022 Meradalir eruption of the Fagradalsfjall Fires, SW-Iceland. *Czech Polar Rep.* **12**, 222–231 (2022).
14. Kahl, M. et al. Deep magma mobilization years before the 2021 CE Fagradalsfjall eruption, Iceland. *Geology* **51**, 184–188 (2023).
15. Flóvenz, Ó. G. et al. Cyclical geothermal unrest as a precursor to Iceland's 2021 Fagradalsfjall eruption. *Nat. Geosci.* **15**, 397–404 (2022).
16. Day, J. M. D. et al. Mantle source characteristics and magmatic processes during the 2021 La Palma eruption. *Earth Planet. Sci. Lett.* **597**, 117793 (2022).
17. Hofmann, A. W., Jochum, K. P., Seufert, M. & White, W. M. Nb and Pb in oceanic basalts: new constraints on mantle evolution. *Earth Planet. Sci. Lett.* **79**, 33–45 (1986).
18. Macpherson, C. G., Hilton, D. R., Day, J. M. D., Lowry, D. & Grönvold, K. High-$^3He/^4He$, depleted mantle and low-$\delta^{18}O$, recycled oceanic lithosphere in the source of central Iceland magmatism. *Earth Planet. Sci. Lett.* **233**, 411–427 (2005).
19. Skovgaard, A. C., Storey, M., Baker, J., Blusztajn, J. & Hart, S. R. Osmium–oxygen isotopic evidence for a recycled and strongly depleted component in the Iceland mantle plume. *Earth Planet. Sci. Lett.* **194**, 259–275 (2001).
20. Huppert, H. E. & Sparks, R. S. J. Cooling and contamination of mafic and ultramafic magmas during ascent through continental crust. *Earth Planet. Sci. Lett.* **74**, 371–386 (1985).
21. Devey, C. W. & Cox, K. G. Relationships between crustal contamination and crystallisation in continental flood basalt magmas with special reference to the Deccan Traps of the Western Ghats, India. *Earth Planet. Sci. Lett.* **84**, 59–68 (1987).
22. Day, J. M. D. Hotspot volcanism and highly siderophile elements. *Chem. Geol.* **341**, 50–74 (2013).
23. Larsen, L. M., Pedersen, A. K., Sundvoll, B. & Frei, R. Alkali picrites formed by melting of old metasomatized lithospheric mantle: Manitdlat Member, Vaigat Formation, Palaeocene of West Greenland. *J. Petrol.* **44**, 3–38 (2003).
24. Weir, N. R. et al. Crustal structure of the northern Reykjanes Ridge and Reykjanes Peninsula, southwest Iceland. *J. Geophys. Res. Solid Earth* **106**, 6347–6368 (2001).
25. Radu, I. B. et al. Water in clinopyroxene from the 2021 Geldingadalir eruption of the Fagradalsfjall Fires, SW-Iceland. *Bull. Volcanol.* **85**, 31 (2023).
26. Day, J. M. D., Walker, R. J. & Warren, J. M. ^{186}Os–^{187}Os and highly siderophile element abundance systematics of the mantle revealed by abyssal peridotites and Os-rich alloys. *Geochim. Cosmochim. Acta* **200**, 232–254 (2017).
27. Blusztajn, J., Hart, S. R., Ravizza, G. & Dick, H. J. B. Platinum-group elements and Os isotopic characteristics of the lower oceanic crust. *Chem. Geol.* **168**, 113–122 (2000).
28. Peucker-Ehrenbrink, B., Bach, W., Hart, S. R., Blusztajn, J. S. & Abbruzzese, T. Rhenium-osmium isotope systematics and platinum group element concentrations in oceanic crust from DSDP/ODP Sites 504 and 417/418. *Geochem. Geophys. Geosyst.* **4**, 8911 (2003).
29. Foulger, G. R. Older crust underlies Iceland. *Geophys. J. Int.* **165**, 672–676 (2006).
30. Torsvik, T. H. et al. Continental crust beneath southeast Iceland. *Proc. Natl Acad. Sci.* **112**, E1818–E1827 (2015).
31. Dale, C. W. et al. Highly siderophile element behaviour accompanying subduction of oceanic crust: whole rock and mineral-scale insights from a high-pressure terrain. *Geochim. Cosmochim. Acta* **73**, 1394–1416 (2009).
32. Heinonen, J. S., Luttinen, A. V., Spera, F. J. & Bohrson, W. A. Deep open storage and shallow closed transport system for a continental flood basalt sequence revealed with Magma Chamber Simulator. *Contrib. Mineral. Petrol.* **174**, 1–18 (2019).
33. Gleeson, M. L., Lissenberg, C. J. & Antoshechkina, P. M. Porosity evolution of mafic crystal mush during reactive flow. *Nat. Commun.* **14**, 3088 (2023).
34. Thirlwall, M. F. et al. Low $\delta^{18}O$ in the Icelandic mantle and its origins: evidence from Reykjanes Ridge and Icelandic lavas. *Geochim. Cosmochim. Acta* **70**, 993–1019 (2006).
35. Hartley, M. & Maclennan, J. Magmatic densities control erupted volumes in Icelandic volcanic systems. *Front. Earth Sci.* **6**, 29 (2018).
36. Condomines, M. et al. Helium, oxygen, strontium and neodymium isotopic relationships in Icelandic volcanics. *Earth Planet. Sci. Lett.* **66**, 125–136 (1983).
37. Pedersen, G. B. et al. Lava flow hazard modelling during the 2021 Fagradalsfjall eruption, Iceland: applications of MrLavaLoba. *Nat. Hazards Earth Syst. Sci. Discuss.* **2022**, 1–38 (2022).
38. Árnadóttir, T., Geirsson, H. & Jiang, W. Crustal deformation in Iceland: plate spreading and earthquake deformation. *Jökull* **58**, 59–74 (2008).
39. Momme, P., Óskarsson, N. & Keays, R. R. Platinum-group elements in the Icelandic rift system: melting processes and mantle sources beneath Iceland. *Chem. Geol.* **196**, 209–234 (2003).
40. Nicklas, R. W., Brandon, A. D., Waight, T. E., Puchtel, I. S. & Day, J. M. D. High-precision Pb and Hf isotope and highly siderophile element abundance systematics of high-MgO Icelandic lavas. *Chem. Geol.* **582**, 120436 (2021).

Methods

Bulk rock major, minor and trace-element abundance determinations

Major-element analyses were completed by X-ray fluorescence at Activation Laboratories Ltd. using their research-grade package 4LITHORES, using the same method as in ref. 5. After fusion with lithium metaborate/tetraborate and digestion in nitric acid, major elements were measured by inductively coupled plasma optical emission spectroscopy. Detection limits are 0.01 wt% for all major-element oxides, except for MnO and TiO, which have detection limits of 0.001 wt%. Data quality was verified by repeated analysis of internal reference materials and analytical precision is estimated at better than 5% for major elements.

Bulk rock minor-element and trace-element abundance data were determined at the Scripps Isotope Geochemistry Laboratory (SIGL), Scripps Institution of Oceanography in a single measurement campaign. Samples were sawn, surfaces cleaned and then approximately 100 g of material was disaggregated using an alumina crusher. The crushed material was then coned-and-quartered and about 30–40 g of material was turned to a fine (sub-10 μm) rock flour using a SPEX alumina shatterbox. For trace-element abundances, approximately 100 mg of sample powder was digested in 4:1 Teflon-distilled concentrated 27 M HF and 15 M HNO_3 for >72 h on a hotplate at 150 °C, along with total procedural blanks and terrestrial basalt and andesite standards (BHVO-2, BCR-2, BIR-1a, AGV-2). Samples were sequentially dried and taken up in concentrated HNO_3 to destroy fluorides. After ensuring complete dissolution, the samples were doped with indium to monitor instrumental drift during analysis and then diluted to a factor of 5,000. Major-element and trace-element abundances were determined using a Thermo Scientific iCAP Qc quadrupole inductively coupled plasma mass spectrometer in normal mode and all data are blank-corrected. Reference materials were analysed as unknowns to assess external reproducibility and accuracy (see also refs. 41,42). Reproducibility was generally better than 5% relative s.d. (Supplementary Data Table 2).

HSE abundance and Re–Os isotope determinations

A subset of the 2021 and 2022 Fagradalsfjall Fires samples analysed for trace-element abundances at Scripps Institution of Oceanography were analysed for Re–Os isotope and HSE abundance analyses. Selection of samples was based primarily on Ni contents, with quantities of isotopically enriched spike added appropriately based on previous HSE abundance analyses of Iceland lavas[39,40]. Osmium isotope and HSE abundance analyses were performed at the SIGL. Homogenized approximately 1 g powder aliquots were digested in sealed borosilicate Carius tubes with an isotopically enriched multielement spike mix (^{99}Ru, ^{106}Pd, ^{185}Re, ^{190}Os, ^{191}Ir, ^{194}Pt) and 11 ml of a 1:2 mixture of multiply Teflon distilled HCl and HNO_3 that was purged with H_2O_2 to remove Os. Samples were digested in Carius tubes to a maximum temperature of 250 °C in an oven for 72 h. Osmium was triply extracted from the acid using CCl_4 and then back-extracted into HBr, before purification by double microdistillation, with the other HSE being recovered and purified from the residual solutions using anion exchange separation[43]. Isotopic compositions of Os were measured in negative-ion mode on a Thermo Scientific Triton thermal ionization mass spectrometer. Re, Pd, Pt, Ru and Ir were measured using a CETAC Aridus II desolvating nebulizer coupled to a Thermo Scientific iCAP Qc ICP-MS. Offline corrections for Os involved an oxide correction, an iterative fractionation correction using ^{192}Os/^{188}Os = 3.08271, a ^{190}Os spike subtraction, a Re interference correction and, finally, an Os blank subtraction. Precision for ^{187}Os/^{188}Os, determined by measurement of a 35 pg UMCP Johnson Matthey standard over the campaign period, was ±0.2% (2 s.d.; 0.11387 ± 24; n = 6). All reported ^{187}Os/^{188}Os data are uncorrected for Re interference, as background ^{185}Re counts did not exceed 5 counts per second.

Measured Re, Ir, Pt, Pd and Ru isotopic ratios for sample solutions were corrected for mass fractionation using the deviation of the standard average run on the day over the natural ratio for the element. External reproducibility on HSE analyses using the iCAP Qc was better than 2% for 0.5 ng solutions for Re, Pd, Pt, Ru and Ir and all reported values are blank-corrected. The total procedural blanks (n = 2) run with the samples had ^{187}Os/^{188}Os = 0.145 to 0.155 ± 0.01, with quantities (in picograms) of 4 (Re), 2–7 (Pd), 10–12 (Pt), 145–190 (Ru), 0.2–0.6 (Ir) and 0.6 (Os). All data are blank-corrected, with the blanks representing ≪5% for Pd, Pt, Ir and Os, <15% for Re and <50% for Ru.

Measurement of ^{187}Os/^{188}Os and HSE abundances for standard reference material BHVO-2

Isotope dilution measurements of the United States Geological Survey standard reference material BHVO-2 were performed with Fagradalsfjall Fires samples (Supplementary Data Table 3). BHVO-2 is a low-abundance basalt standard reference material and has been analysed in numerous studies (for example, refs. 44–47) and has also been reported in previous studies from the SIGL[48,49]. Four separate digestions of BHVO-2 (powder aliquot #1955) are reported for this study and, together with data from refs. 46,47, show average reproducibility for ^{187}Os/^{188}Os of about 3 RSD%, with abundance reproducibility of 4 RSD% for Re and 23–62 RSD% for Pd, Pt, Ru, Ir and Os. This reproducibility is equal to or better than that for the combined data from previously published studies and demonstrates that absolute abundance variability can be notable in some basaltic lava flows, especially in the case of BHVO-2, for Pt.

Comparison with absolute abundances reported from previous studies shows that BHVO-2 data from the SIGL are marginally higher for Re, Pd, Ru, Ir and Os (Supplementary Data Table 3 and Extended Data Fig. 5). This may relate to variability within powder aliquots provided by the United States Geological Survey or it could relate to digestion procedures, at which higher abundances of these elements would equate to more efficient digestion. In the case of this study, it does not relate to the isotopically enriched spike that was calibrated during the analytical campaign.

Are the 2021 Fagradalsfjall Fires lavas anomalous with respect to Os isotope composition?

The earliest Fagradalsfjall Fires lavas have radiogenic ^{187}Os/^{188}Os and typically have Os contents >50 pg g^{-1}. Compared with Icelandic lavas measured previously for Os isotope compositions and abundances, the earliest Fagradalsfjall Fires are highly radiogenic, especially if only lavas with >50 pg g^{-1} are considered (Extended Data Fig. 1, containing refs. 50–57). It is typically assumed that OIB lavas with Os contents greater than 30–50 pg g^{-1} are less susceptible to the effects of contamination (for example, refs. 22,58). It is important to note in this regard that, although every location should be considered individually to assess local potential crust assimilants, these previous studies of OIB and of published Icelandic lavas have measured samples that erupted long before their collection, sometimes as much as >1 Ma or more (for example, lavas from the Miocene volcanic rocks of northwest Iceland[50]). The 30–50 pg g^{-1} cut-off threshold therefore also partially accounts for ingrowth of Os, especially in samples with low Os contents and high Re/Os.

For Iceland, 50 pg g^{-1} is a highly conservative cut-off, given that >98% of published Iceland data with >10 pg g^{-1} has ^{187}Os/^{188}Os < 0.14, within the average of published Iceland lavas with >50 pg g^{-1} and ^{187}Os/^{188}Os from 0.1263 to 0.1419. These relationships show how anomalous the beginning lavas of 2021 from the Fagradalsfjall Fires lavas are for Os isotopic composition. As shown in the main text, this anomalous Os isotope composition between the 2021 and 2022 instalments of the Fagradalsfjall Fires directly reflects deep crustal assimilation not previously observed in Iceland or elsewhere at other OIB localities.

Fractional crystallization and assimilation modelling

Models to explore possible extents of fractional crystallization and crustal assimilation were examined for the presented Os isotope and HSE abundance data, for previously reported Sr–Nd–Pb isotope data for the first 50 days of the 2021 Fagradalsfjall Fires eruption[7], as well as O isotope data. Model parameters for the models shown in Fig. 4 and Extended Data Figs. 2 and 4 (containing refs. 59–62) are given in Supplementary Data Table 4. Parameters for the models in Extended Data Fig. 3 are provided in the figure caption. The extremely radiogenic $^{187}Os/^{188}Os$ in Fagradalsfjall Fires lavas was unexpected, prompting consideration of extreme contaminants, from ancient, recycled ocean crust or continental lithospheric mantle in the plume itself, to assimilation of high Re + Pt/Ir + Os sulfides. In this context, it is worth emphasizing that very high Re/Os is required to be isolated from magma sources to generate the radiogenic $^{187}Os/^{188}Os$ in the earliest 2021 Fagradalsfjall Fires lavas regardless of source. Typically, this would be assumed to be crystallized magmatic products with high Re/Os, although we also explore the possibility that crystal mushes with high-Re/Os sulfide may also have been capable of generating similar signatures.

Comparison with previous plumbing system models

To place the results of this work into context, we present Extended Data Fig. 6, showing how the Os isotope data can be considered in the context of the Fagradalsfjall Fires.

Supplementary data table summary

Supplementary Data Table 1 presents new Re–Os isotope and HSE abundance data for the 2021 and 2022 lavas of the Fagradalsfjall Fires. Supplementary Data Table 2 presents new trace-element abundance data for the same samples. Supplementary Data Table 3 presents new and previously published BHVO-2 standard reference material data. Supplementary Data Table 4 shows model parameters for figures, including refs. 63–66.

Data availability

Source data are provided with this paper in the Supplementary Information and tables. The data are also available at EarthChem (https://doi.org/10.60520/IEDA/113167).

41. Day, J. M. D., Peters, B. J. & Janney, P. E. Oxygen isotope systematics of South African olivine melilitites and implications for HIMU mantle reservoirs. *Lithos* **202**, 76–84 (2014).
42. Tait, K. T. & Day, J. M. D. Chondritic late accretion to Mars and the nature of shergottite reservoirs. *Earth Planet. Sci. Lett.* **494**, 99–108 (2018).
43. Day, J. M. D., Waters, C. L., Schaefer, B. F., Walker, R. J. & Turner, S. Use of hydrofluoric acid desilicification in the determination of highly siderophile element abundances and Re-Pt-Os isotope systematics in mafic-ultramafic rocks. *Geostand. Geoanal. Res.* **40**, 49–65 (2016).
44. Meisel, T. & Moser, J. Platinum group element and rhenium concentrations in low abundance reference materials. *Geostand. Geoanal. Res.* **28**, 233–250 (2004).
45. Shinotsuka, K. & Suzuki, K. Simultaneous determination of platinum group elements and rhenium in rock samples using isotope dilution inductively coupled plasma mass spectrometry after cation exchange separation followed by solvent extraction. *Anal. Chim. Acta* **603**, 129–139 (2007).
46. Li, J. et al. Determination of platinum-group elements and Re-Os isotopes using ID-ICP-MS and N-TIMS from a single digestion after two-stage column separation. *Geostand. Geoanal. Res.* **38**, 37–50 (2013).
47. Chu, Z. et al. A comprehensive method for precise determination of Re, Os, Ir, Ru, Pt, Pd concentrations and Os isotopic compositions in geological samples. *Geostand. Geoanal. Res.* **39**, 151–169 (2014).
48. Day, J. M. D., Nutt, K. L., Mendenhall, B. & Peters, B. J. Temporally variable crustal contributions to primitive mantle-derived Columbia River Basalt Group magmas. *Chem. Geol.* **572**, 120197 (2021).
49. Durkin, K., Day, J. M. D., Panter, K. S., Xu, J.-F. & Castillo, P. R. Petrogenesis of alkaline magmas across a continent to ocean transect, northern Ross Sea, Antarctica. *Chem. Geol.* **641**, 121780 (2023).
50. Mundl-Petermeier, A. et al. Temporal evolution of primordial tungsten-182 and $^{3}He/^{4}He$ signatures in the Iceland mantle plume. *Chem. Geol.* **525**, 245–259 (2019).
51. Martin, C. E. Osmium isotopic characteristics of mantle-derived rocks. *Geochim. Cosmochim. Acta* **55**, 1421–1434 (1991).
52. Pegram, W. J. & Allègre, C. J. Osmium isotopic compositions from oceanic basalts. *Earth Planet. Sci. Lett.* **111**, 59–68 (1992).
53. Roy-Barman, M. & Allègre, C. J. $^{187}Os/^{186}Os$ in oceanic island basalts: tracing oceanic crust recycling in the mantle. *Earth Planet. Sci. Lett.* **129**, 145–161 (1995).
54. Jackson, M. G. et al. Globally elevated titanium, tantalum, and niobium (TITAN) in ocean island basalts with high $^{3}He/^{4}He$. *Geochem. Geophys. Geosyst.* **9**, Q04027 (2008).
55. Debaille, V. et al. Primitive off-rift basalts from Iceland and Jan Mayen: Os-isotopic evidence for a mantle source containing enriched subcontinental lithosphere. *Geochim. Cosmochim. Acta* **73**, 3423–3449 (2009).
56. Brandon, A. D., Graham, D. W., Waight, T. & Gautason, B. ^{186}Os and ^{187}Os enrichments and high-$^{3}He/^{4}He$ sources in the Earth's mantle: evidence from Icelandic picrites. *Geochim. Cosmochim. Acta* **71**, 4570–4591 (2007).
57. Smit, Y. *The Snaefellsnes Transect: A Geochemical Cross-section Through the Iceland Plume*. PhD thesis, Open University (2004).
58. Reisberg, L. et al. Os isotope systematics in ocean island basalts. *Earth Planet. Sci. Lett.* **120**, 149–167 (1993).
59. Eiler, J. M., Grönvold, K. & Kitchen, N. Oxygen isotope evidence for the origin of chemical variations in lavas from Theistareykir volcano in Iceland's northern volcanic zone. *Earth Planet. Sci. Lett.* **184**, 269–286 (2000).
60. Slater, L., McKenzie, D., Gronvold, K. & Shimizu, N. Melt generation and movement beneath Theistareykir, NE Iceland. *J. Petrol.* **42**, 321–354 (2001).
61. Breddam, K. Kistufell: primitive melt from the Iceland mantle plume. *J. Petrol.* **43**, 345–373 (2002).
62. Peate, D. W. et al. Historic magmatism on the Reykjanes Peninsula, Iceland: a snap-shot of melt generation at a ridge segment. *Contrib. Mineral. Petrol.* **157**, 359–382 (2009).
63. Day, J. M. D., Pearson, D. G., Macpherson, C. G., Lowry, D. & Carracedo, J. C. Evidence for distinct proportions of subducted oceanic crust and lithosphere in HIMU-type mantle beneath El Hierro and La Palma, Canary Islands. *Geochim. Cosmochim. Acta* **74**, 6565–6589 (2010).
64. Luguet, A. et al. Enriched Pt-Re-Os isotope systematics in plume lavas explained by metasomatic sulfides. *Science* **319**, 453–456 (2008).
65. Kempton, P. D. & Hunter, A. G. A Sr-, Nd-, Pb-, O-isotope study of plutonic rocks from MARK, Leg 153: implications for mantle heterogeneity and magma chamber processes. Ocean Drilling Program Scientific Results Leg 153 - Mid-Atlantic Ridge, 305–319 (1997).
66. Coogan, L. A. The lower oceanic crust. *Treatise Geochem.* **2**, 497–541 (2014).

Acknowledgements Financial support came from NSF EAR 1918322 (J.M.D.D.) and from the Swedish Research Council and the European Research Council synergy grant (ERC-2023-SyG101118491) (V.R.T.). We are grateful to S. A. Halldorsson for comments that focused arguments in this work.

Author contributions W.M.M., V.R.T. and T.T. collected samples. J.M.D.D., S.K. and V.R.T. prepared and analysed all rock samples. J.M.D.D. wrote the first version of the manuscript, with critical input from all authors. All authors contributed to data interpretations, critical discussions and commented on the manuscript.

Competing interests The authors declare no competing interests.

Additional information

Supplementary information The online version contains supplementary material available at https://doi.org/10.1038/s41586-024-07750-0.

Correspondence and requests for materials should be addressed to James M. D. Day.

Peer review information *Nature* thanks Adam Kent, Holly Stein and the other, anonymous, reviewer(s) for their contribution to the peer review of this work. Peer reviewer reports are available.

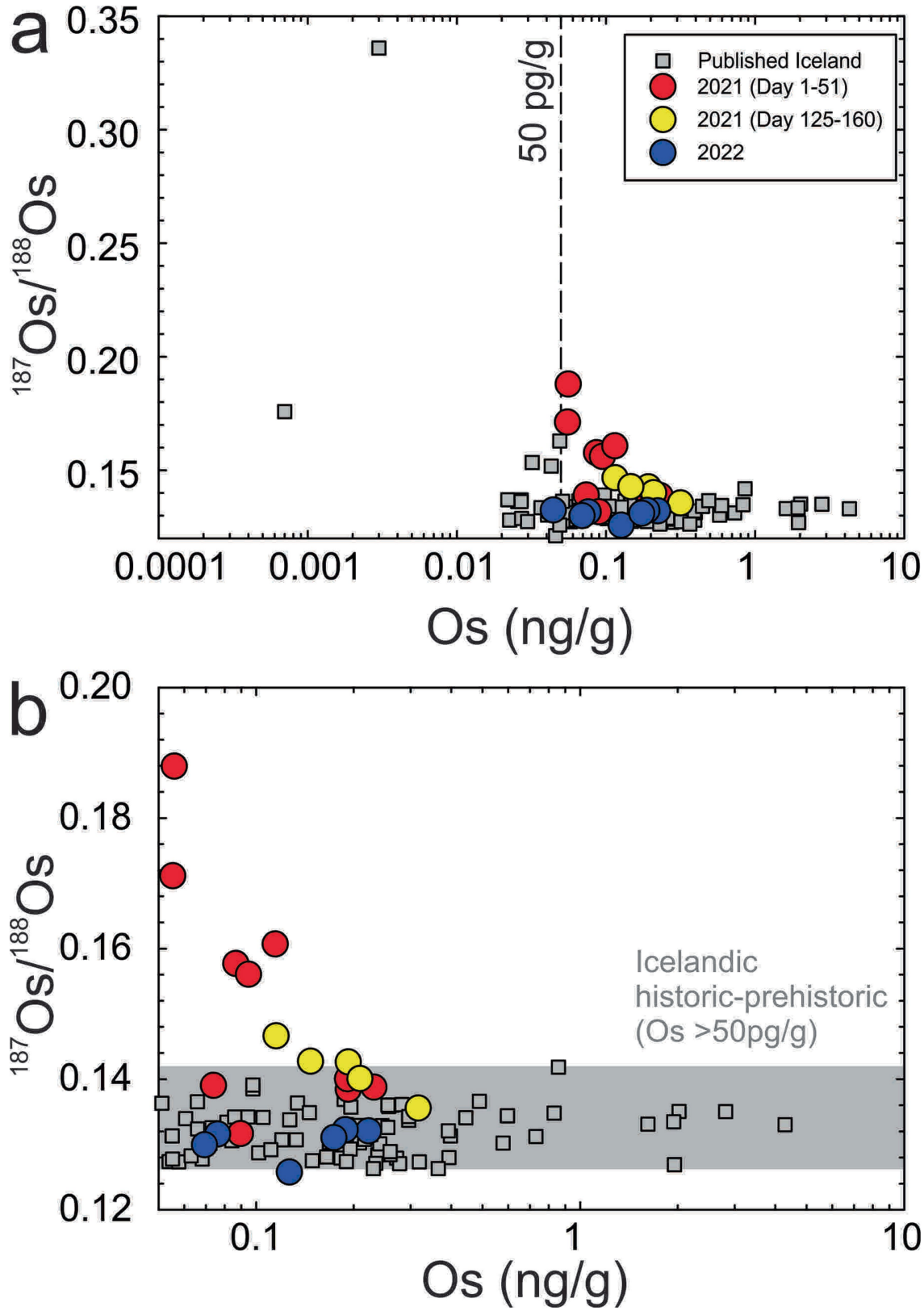

Extended Data Fig. 1 | Plots of Os abundance versus Os isotope composition from Icelandic basalts. Data are from this study and refs. 19,40,50–57. **a**, The conservative 50 pg g^{-1} (or pg/g) cut-off for OIB lavas[22]. **b**, Data are all Icelandic historic or prehistoric samples of lavas with >50 pg g^{-1} Os, defining a range of $^{187}Os/^{188}Os$ ratios from 0.1263 to 0.1419 (average = 0.1320 ± 0.0072, 2 s.d). The most radiogenic high-Os samples outside the Fagradalsfjall Fires are from the Miocene volcanic rocks of northwest Iceland (ICE-14-16/18 from ref. 50) and so may be subject to notable age corrections. Note the anomalous compositions of the earliest 2021 Fagradalsfjall Fire lavas and the general correspondence of low Os contents with radiogenic $^{187}Os/^{188}Os$ in the 2021 eruption but not in the 2022 eruption.

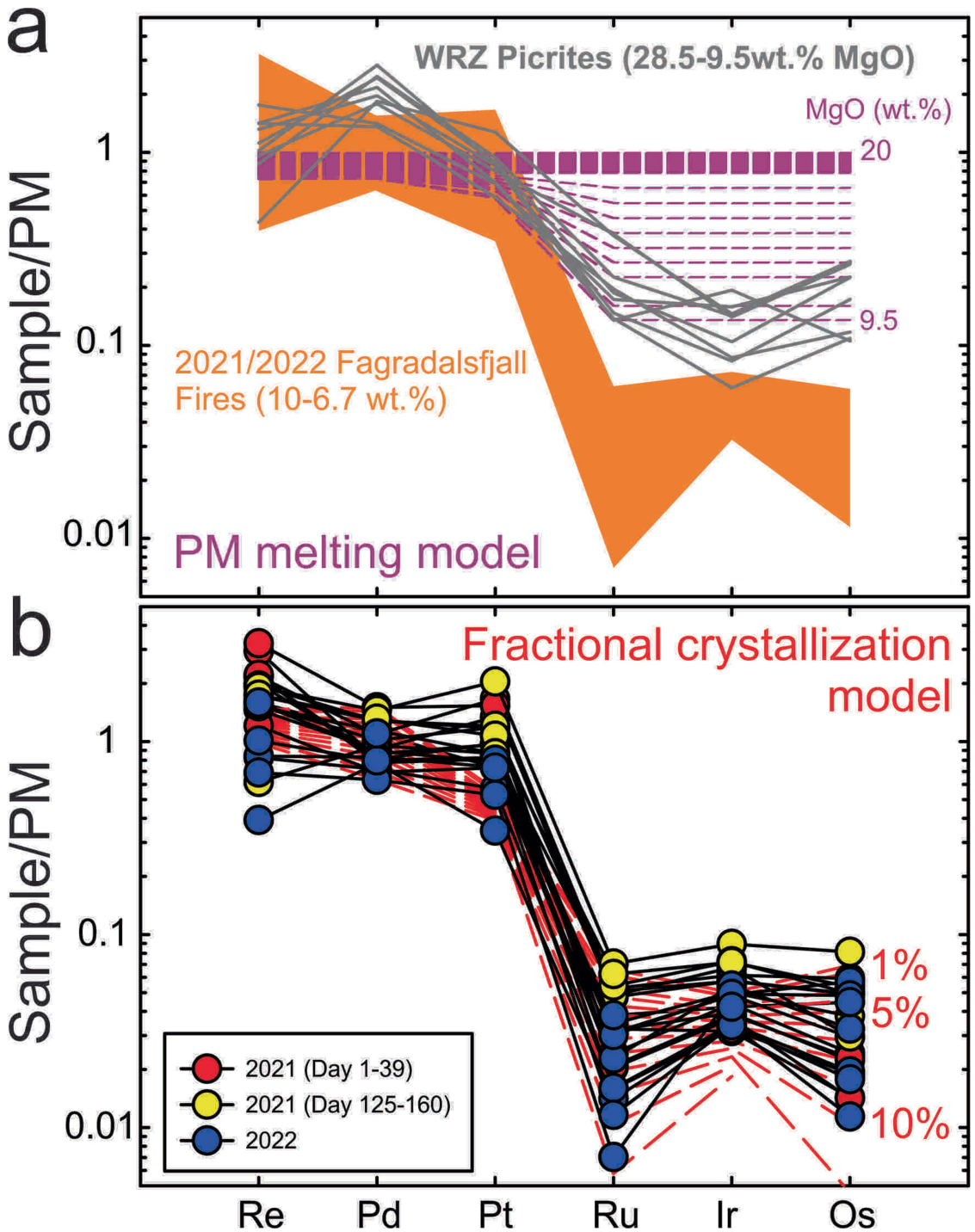

Extended Data Fig. 2 | Primitive mantle-normalized HSE diagrams. a, Field of lavas for the 2021 and 2022 Fagradalsfjall Fires versus HSE patterns for prehistoric Icelandic lavas with 9.5–28.0 wt% MgO from ref. 40. Shown is a fractional crystallization model of a primary primitive mantle melt (purple lines) showing compositional variations expected during crystallization. **b**, Individual 2021 and 2022 Fagradalsfjall Fires HSE patterns versus a model of Ol + Cr + S crystal (red lines) shows the results for 0 to >12% olivine crystallization with co-crystallization of Cr-spinel and sulfide, in the proportions 0.98 olivine, 0.019 Cr-spinel and 0.001 sulfide, using partition coefficients and starting compositions given in Supplementary Data Table 4.

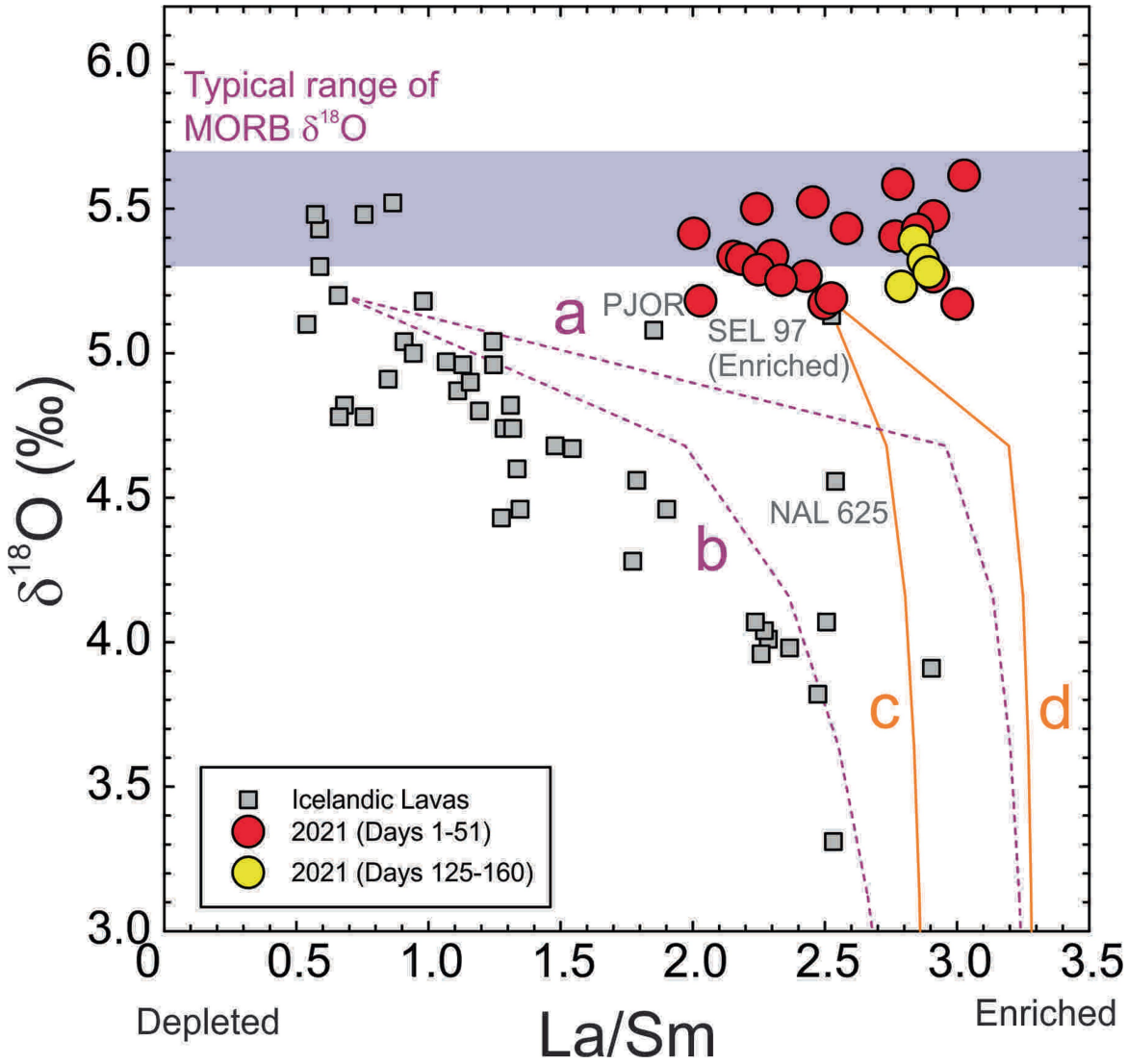

Extended Data Fig. 3 | Plot of $\delta^{18}O_{melt}$ versus La/Sm. Oxygen isotope ratios are plotted as bulk samples (2021 Fagradalsfjall Fires), glass $\delta^{18}O$ values or, when olivine was analysed, as melt equivalent based on $\Delta_{melt\text{-}ol}$ of +0.4‰. Curves a and b represent mixing between a depleted melt with $\delta^{18}O$ = +5.2‰ and La/Sm = 0.67 with Krafla basalt with La = 6.3 μg g^{-1} and La/Sm = 2.9, with $\delta^{18}O$ = 0‰ (a) and rhyolitic magma with $\delta^{18}O$ = 0‰, with La = 30 μg g^{-1} and La/Sm = 3.3 (b). Curves c and d are for mixing with the same shallow-level crustal contaminants as given in a and b, respectively, but with a starting melt composition with La/Sm = 2.5 and $\delta^{18}O$ = +5.2‰. High-$^{3}He/^{4}He$ 'enriched' picrites from northwest Iceland (SEL 97) and central Iceland (NAL 625, PJOR) are shown from ref. 18. Models and published Iceland data (Icelandic lavas) are from refs. 18,19,59–61. The O isotope data from ref. 19 have been replaced by that from ref. 34. Note that even the most depleted Fagradalsfjall Fires lavas are not as depleted as some central Icelandic lavas with La/Sm < 1. Later Fagradalsfjall Fires lavas stored at upper crustal depths probably have low-$\delta^{18}O$ signatures based on models c and d.

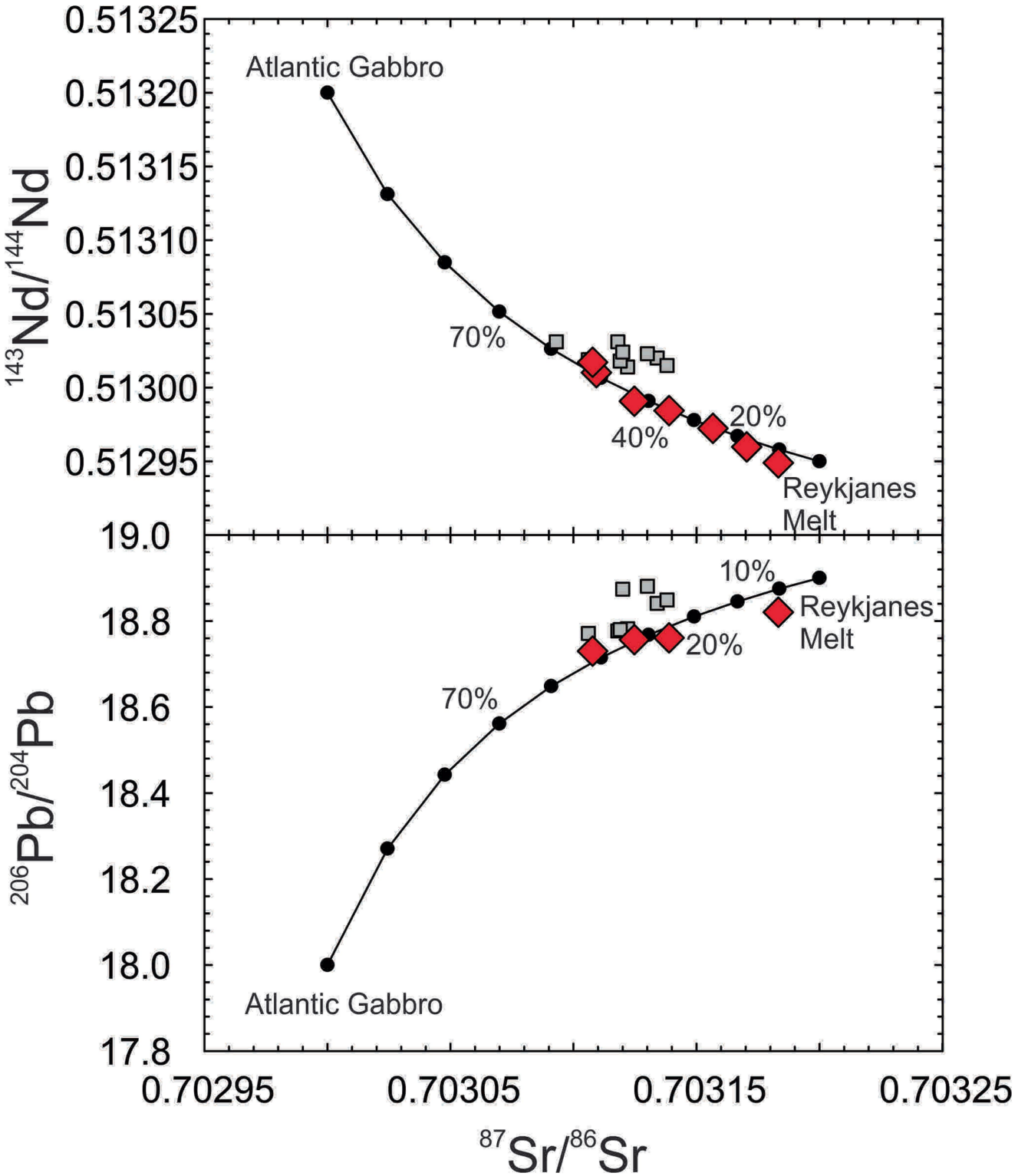

Extended Data Fig. 4 | Examples of assimilation of Atlantic gabbro (depleted source of Sr, Nd and Pb) by the early 2021 Fagradalsfjall Fires lavas. Osmium isotope data indicate that high quantities of assimilated oceanic crust with high Re/Os is permissible, consistent with up to 20% assimilation of such material from Sr–Nd–Pb isotopes. Data in red diamonds and grey squares are from refs. 7,62, respectively, and model parameters and sources are given in Supplementary Data Table 4.

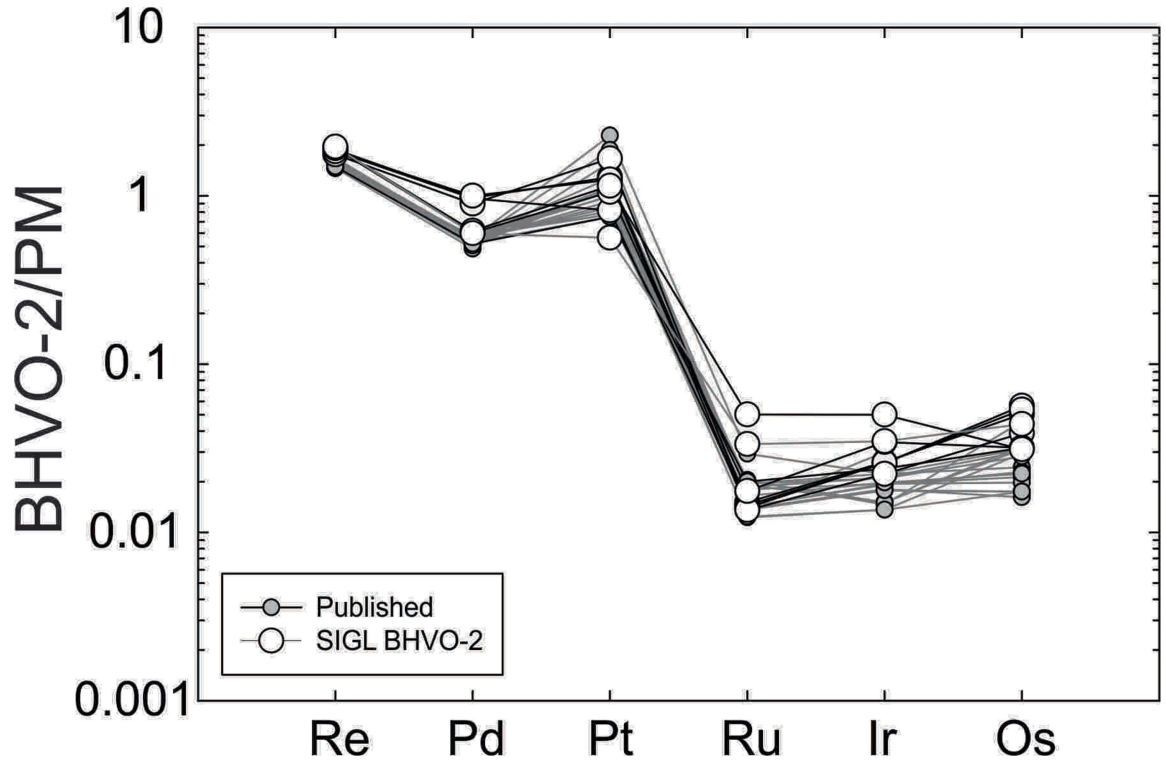

Extended Data Fig. 5 | Primitive mantle-normalized HSE diagram for the BHVO-2 standard reference material. Data from this study and other reported values from the SIGL[48,49] are shown versus published data[44–47]. Primitive mantle normalization from ref. 26.

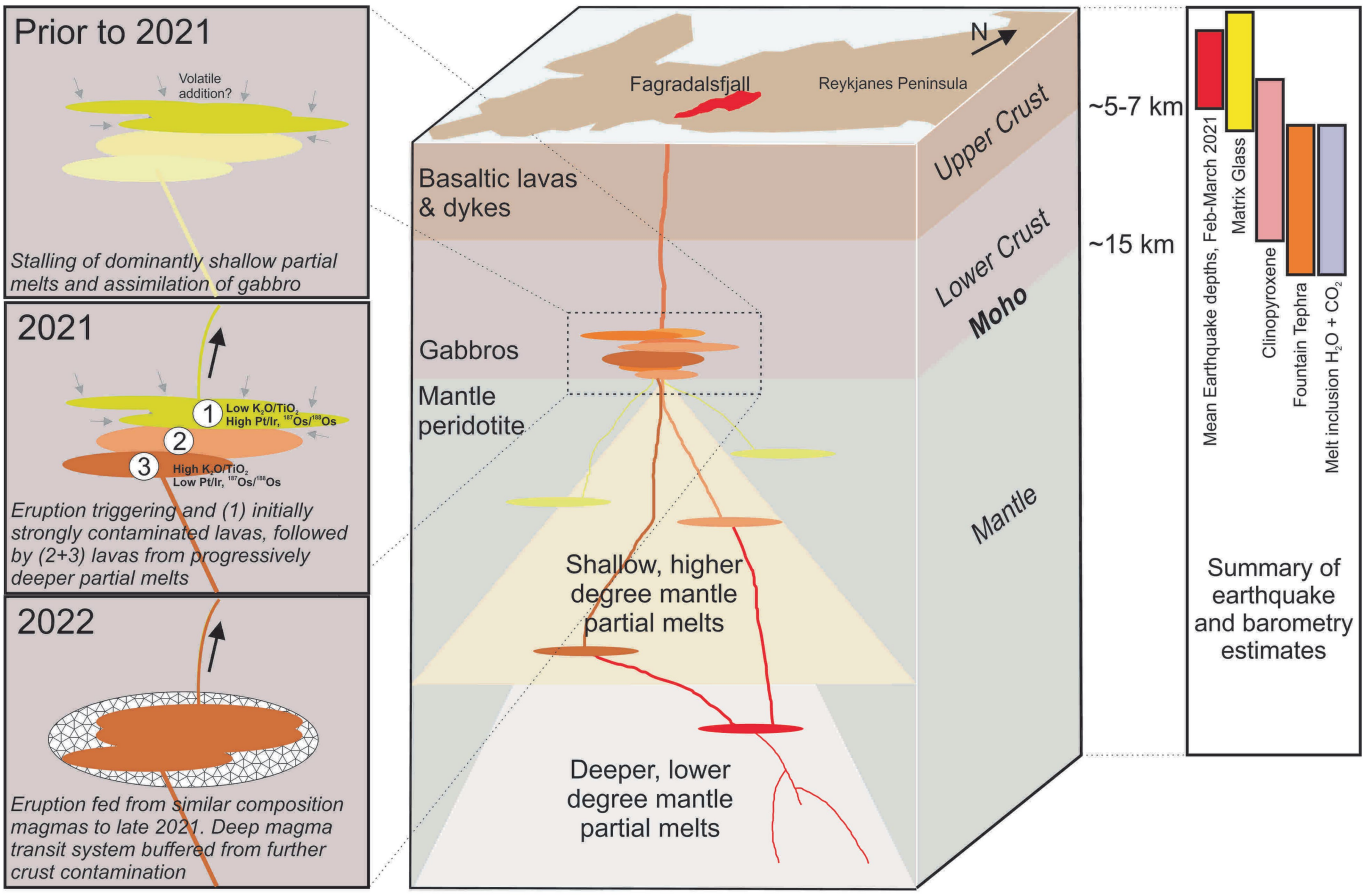

Extended Data Fig. 6 | A potential model for the magma plumbing system beneath Fagradalsfjall Fires. Initially, parental magmas originated from polybaric melting to shallow levels, followed by fractional crystallization. Magmas migrated above the Moho in late 2020, at which they fractionated olivine ± clinopyroxene + Cr-spinel + sulfide before eventual mobilization in March 2021. Here they were contaminated by high-Re/Os and high-Pt/Ir melts. As the eruption progressed, progressively deeper portions of the underplating magma feeding zone were involved in the eruption, as suggested by ref. 7. Shown are barometry estimates for crystallization pressures from refs. 7,25 and earthquake focal depth data are summarized from ref. 6.